SAND2014-1968C

Considering DIC Uncertainties in Material Property Identification Using VFM

Sharlotte Kramer, William Scherzinger, Phillip Reu, and Miguel Aguilo
Sandia National Laboratories

Abstract

Inverse problem methodologies for material property identification often rely on full-field experimental measurements from optical methods. These vital measurements have experimental errors that can lead to large uncertainties in the identified properties, particularly in inverse approaches that utilize nonlinear iterative optimization algorithms where experimental error can lead to spurious local minima. In this paper, the effects of uncertainties associated with Digital Image Correlation (DIC) displacement measurements are investigated for a finite deformation Virtual Fields Method (VFM) approach for plasticity model parameter identification. The complete VFM inverse problem methodology is simulated using computationally derived displacements with superimposed DIC measurement uncertainties, which were quantified for representative DIC experimental setups, as inputs to the identification algorithm. The simulated VFM process that incorporates measurement errors allows for characterizing the impact of DIC uncertainties based on realistic experimental parameters without requiring cost-prohibitive iterative experimental investigations of the full VFM process. This study can help with specimen-geometry and DIC-setup designs so that the real experiments provide optimal measurements for lower uncertainties in finite deformation VFM material property identification.

The Virtual Fields Method for Finite Deformation

The Virtual Fields Method (VFM) is an approach to constitutive model parameter identification that utilizes full-field deformation measurements and the Principle of Virtual Work [1]. VFM has been applied to large-deformation plasticity [2] using a nonlinear minimization process with the Principle of Virtual Power for finite deformations. The Principle of Virtual Power in terms of the Lagrangian description, assuming quasi-static loading and no body forces, is:

$$\int_{V_o} \mathbf{\Pi}^T : \delta\dot{\mathbf{F}}\, dV = \int_{\partial V_o} (\mathbf{\Pi}^T \boldsymbol{n}_o)\cdot \delta\mathbf{v}\, dS \tag{1}$$

where $\mathbf{\Pi}$ is the first Piola-Kirchoff stress tensor, $\delta\dot{\mathbf{F}} = \nabla\delta\mathbf{v}(\boldsymbol{x}_o, t)$ is the virtual velocity gradient tensor, ∂V_o is the boundary of the reference volume V_o, $\boldsymbol{n}_o$ is the surface normal in the undeformed configuration, and $\delta\mathbf{v}$ is a kinematically admissible velocity vector field. The purpose of VFM is to identify a constitutive parameter set ξ from measured full-field displacements and applied loads for heterogeneous stress states during the course of a test. By choosing kinematically admissible virtual velocity fields and appropriately managing the nonlinear VFM problem for the case of a nonlinear constitutive model, the user can identify ξ by minimizing the following cost function $\Phi(\xi)$:

$$\Phi(\xi) = \sum_{i=1}^{N_{vf}} \sum_{j=1}^{N_{step}} \Big[\int_{V_o} \mathbf{\Pi}_j^T : \delta\dot{\mathbf{F}}_i\, dV - \int_{\partial V_o} (\mathbf{\Pi}_j^T \boldsymbol{n}_o)\cdot \delta\mathbf{v}_i\, dS \Big]^2 \tag{2}$$

where N_{vf} is the number of virtual fields, and N_{step} is the number of measurement steps. Eq. (2) is the balance of the internal virtual power in the volume and the external virtual power on the boundary. By using a plasticity model in the cost function $\Phi(\xi)$ with measured displacements and appropriate virtual velocities, the minimization process of $\Phi(\xi)$ returns values for the unknown parameters set ξ.

A quasi-Newton optimization algorithm in the Design Optimization Toolkit (DOTk) [3] was employed to minimize the objective function. In quasi-Newton methods, the Hessian is updated by analyzing successive gradient vectors instead of computing the Hessian matrix. A limited memory Broyden, Fletcher, Goldfarb and Shanno (L-BFGS) method was used to approximate the inverse Hessian operator [4]. The search direction is determined by the product of the inverse Hessian operator and the gradient of the objective function. This computation requires a sequence of inner products and vector summations involving the gradient of the objective function and the pairs of changes in the design variables and objective function gradient, $\{\Delta x_k, \Delta g_k\}$. To approximate the application of the gradient of the objective function to the inverse of the Hessian, the L-BFGS two-loop recursion algorithm was utilized. The gradient of the objective function was approximated via a backward difference approach [5].

Simulated DIC Data

The simulated DIC data used in the VFM identification process is generated through a superposition of experimentally derived uncertainty of position and displacement measurements onto a FEM solution. The DIC errors come from stereo-DIC lab setups of a representative field-of-view (FOV), here approximately 100-mm along one side for a 2448×2048 pixel CCD cameras with 75-mm lenses. The uncertainty of the calibration, position, and displacements are calculated from a combination of experimental images, Correlated Solutions' VIC3D software, and Monte Carlo runs of the DIC analysis process as described in [6]. A large calibration set of images are used to quantify the calibration uncertainties, and the matching error between the two cameras is the error reported by VIC3D software in the calibration. The position error are the standard deviation of the X, Y, and Z locations at each subset of the image. Typically, the positional errors are smaller in the center of the FOV (around 0.0005-mm in X and Y and 0.002-mm in Z) and larger at the edges. The displacement errors are determined using a Monte Carlo approach of images between two positions of the speckle pattern, which was translated approximately 0.5-mm in X, Y, and Z. The displacement errors are the standard deviations of these Monte Carlo runs.

A uniform grid of potential DIC data points are overlaid on a FEM solution at a data density typical of DIC setups (here a step size of 12 pixels for a subset size of 25 pixels.) DIC points are located at the center of the subsets, and the entirety of acceptable subsets must lie inside the speckle pattern on the specimen. To simulate this, each potential DIC subset is tested to determine if it is all on the surface of the FEM mesh, and all unacceptable subsets are eliminated. Fig. 1 shows the front surface of a FEM mesh of an example notched tension specimen and a closeup of the acceptable DIC data points. The FEM displacement solution is sampled at the acceptable simulated DIC subset center points using standard linear shape functions of the FEM elements. Simulated error in u, v, and w at each DIC data point is taken as a random sample from a Gaussian distribution with standard deviation equal to the experimentally measured uncertainties σ_u, σ_v, and σ_w at the corresponding pixel location on the CCD camera. These error values are added to the displacements at each point. The DIC data points are projected back on the FEM mesh nodal locations for the VFM identification process. The scattered DIC points around each node inform each nodal displacement using a basis of piecewise linear functions as used in FEM [7]. This process for simulating the use of DIC data, including data density and experimentally derived error values, will allow for detailed characterization of how using DIC data affects the identification process with the virtual fields method. Additionally, this process allows the user to simulate the experimental parameters such as DIC data density and specimen geometry prior to performing the actual experiments, so the user can optimize these parameters for optimal constitutive parameter identification with VFM.

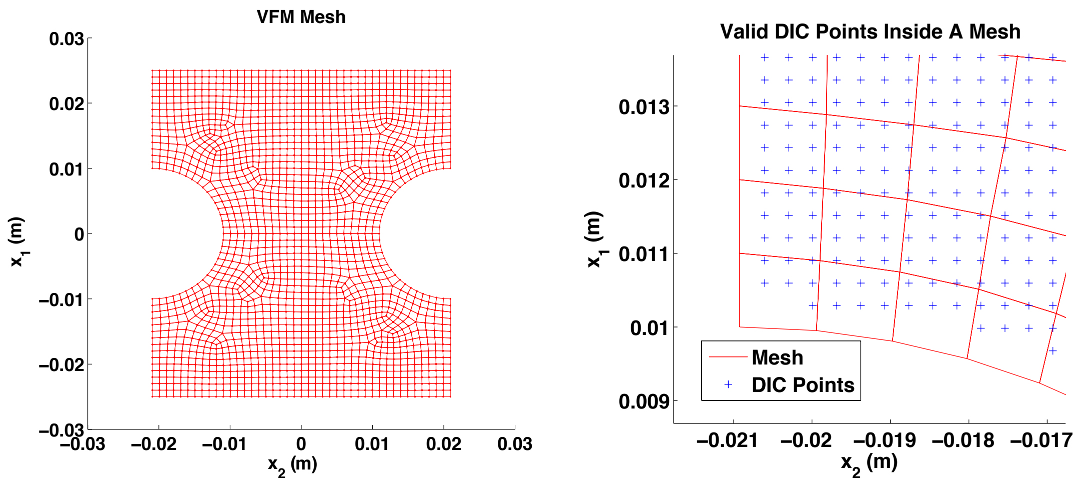

(a) (b)

Figure 1: (a) FEM / VFM mesh of a notched tensile specimen, and (b) closeup of the DIC data points relative to the FEM / VFM mesh.

References

[1] F. Pierron and M. Grediac. *The Virtual Fields Method: Extracting constitutive mechanical parameters from full-field deformation measurements*. Springer, 2012.

[2] M. Rossi and F. Pierron. Identification of plastic consitutive parameters at large deformations from three dimensional dispalcement fields. *Comput. Mech.*, 49:53–71, 2012.

[3] Miguel A. Aguiló. Design Optimization Toolkit: Users' Manual. Sandia report sand2014-5333492, Sandia National Laboratories, Albuquerque, NM, 2014.

[4] J. Nocedal and S. J. Wright. *Numerical Optimization*. Springer, 2006.

[5] D.P. Bertsekas. *Nonlinear Programming*. Athena Scientific, 1999. ISBN 1-886529-00-0.

[6] P.L. Reu. A study of the influence of calibration uncertainty on the global uncertainty for digital image correlation using a monte carlo approach. *Experimental Mechanics*, 53(9):1661–1680, 2013.

[7] J.-H. Kim, A. Serpantié, F. Barlat, F. Pierron, and M.-G. Lee. Characterization of the post-necking strain hardening behavior using the virtual fields method. *Int. J. Solids and Struct.*, 50(24):3829–3842, 2013.